



Cite this: *Org. Biomol. Chem.*, 2024, **22**, 8973

## Total synthesis, stereochemical assignment, and biological evaluation of opantimycin A and analogues thereof†

Yoshinosuke Usuki,<sup>id</sup>\*<sup>a</sup> Ryota Abe,<sup>a</sup> Kazuki Nishiguchi,<sup>a</sup> Tetsuya Satoh,<sup>id</sup><sup>a</sup> Harumi Aono,<sup>b</sup> Toshihiko Nogawa,<sup>b</sup> Yushi Futamura,<sup>id</sup><sup>b</sup> Hiroyuki Osada,<sup>‡</sup><sup>b</sup> Izumi Yoshida,<sup>id</sup><sup>c</sup> Kazuhiro Fujita,<sup>id</sup><sup>c</sup> Takashi Mishima,<sup>id</sup><sup>c</sup> and Ken-Ichi Fujita,<sup>id</sup><sup>d</sup>

Opantimycin A, a rare antimycin-class antibiotic without the macrolide core, was isolated from *Streptomyces* sp. RK88-1355 in 2017. In this study, we explored the total synthesis and stereochemical assignment of opantimycin A. The synthesis of all potential diastereomers has been accomplished *via* traceless Staudinger ligation. A comparison of the spectroscopic data of the synthesized compounds with that reported for the natural product confirmed that the absolute configuration of the natural product was (14*S*,17*R*,21*R*). Two analogous compounds were prepared, where the Dhb ((*Z*)-dehydrobutyrine) moiety was replaced with Dha (dehydroalanine) or  $\Delta$ Val moieties, respectively. The inhibitory activities of these synthetic compounds against the production of the anti-inflammatory cytokine IL-6 were evaluated, and two potential candidates for further development as anti-inflammatory agents were identified.

Received 9th September 2024,  
Accepted 10th October 2024

DOI: 10.1039/d4ob01475h

rsc.li/obc

## Introduction

Opantimycin A (**1**) was isolated from *Streptomyces* sp. RK88-1355 by Osada and co-workers in 2017.<sup>1</sup> This metabolite showed weak antimalarial activity against *Plasmodium falciparum* 3D7 (IC<sub>50</sub>: 13  $\mu$ g mL<sup>-1</sup>). The planar structure of **1** was determined based on 2D NMR analyses and MS/MS experiments, as shown in Fig. 1. Opantimycin A could be classified as an antimycin-type depsipeptide,<sup>2</sup> one of the well-known antifungal metabolites produced by *Streptomyces* sp., as it is composed of  $\gamma$ -butyrolactone, lactate, (*Z*)-2,3-dehydro-2-aminobutyric acid (Dhb), and 3-formylaminosalicylic acid. The NOESY experiment suggested a *cis*-relative configuration for

C17 and C21 on the  $\gamma$ -butyrolactone ring; however, the absolute configuration of the three stereogenic centers could not be elucidated at that time.

Recently, we have achieved the total synthesis of isoneoantimycin (**2**),<sup>3</sup> the first reported acyclic antimycin-class antibiotic with  $\gamma$ -butyrolactone. Considering that threonine residue could be converted to Dhb by  $\beta$ -elimination of the  $\alpha$ -hydroxy- $\beta$ -methyl-valeric acid moiety, the (14*S*,17*R*,21*R*) configuration is the most likely for **1**.

The diverse biological activities of antimycin antibiotics, including anti-cancer, antifungal, and immunosuppressant properties, have attracted significant attention from research-

<sup>a</sup>Department of Chemistry, Graduate School of Science, Osaka Metropolitan University, 3-3-138 Sugimoto, Sumiyoshi, Osaka 558-8585, Japan.  
E-mail: usuki@omu.ac.jp

<sup>b</sup>RIKEN Center for Sustainable Research Science, 2-1 Hirosawa, Wako, Saitama 351-0198, Japan

<sup>c</sup>Saito Laboratory, Japan Food Research Laboratories, 4-41 Saito-asagi 7-chome, Ibaraki-shi, Osaka 567-0085, Japan

<sup>d</sup>Department of Biology, Graduate School of Science, Osaka Metropolitan University, 3-3-138 Sugimoto, Sumiyoshi, Osaka 558-8585, Japan

† Electronic supplementary information (ESI) available: Comparisons of the NMR data of natural and synthetic compounds (Tables SI1–4 and Fig. SI1 and 2), UPLC analysis (Fig. SI-3), experimental details and spectra, biological evaluations against IL-6 gene expression and cell viability in RAW264 cells (Fig. SI4 and 5). See DOI: <https://doi.org/10.1039/d4ob01475h>

‡ Present address: Institute of Microbial Chemistry (BIKAKEN), 3-14-23 Kamiosaki, Shinagawa-ku, Tokyo 141-0021, Japan.

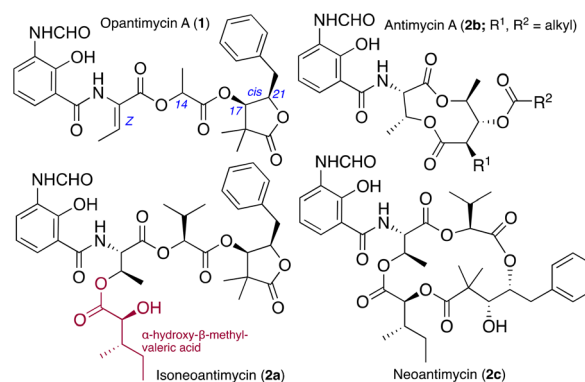


Fig. 1 Structures of opantimycin A (**1**), isoneoantimycin (**2a**), antimycin A (**2b**) and neoantimycin (**2c**).



ers.<sup>4</sup> In particular, neoantimycins and their homologues, the ring-expanded antimycins, have been shown to be effective regulators of the oncogenic proteins GRP78/BiP and K-Ras.<sup>5</sup>

During our investigation of antimycin-type antibiotics,<sup>6</sup> we conducted studies aimed at the synthetic elucidation of the stereochemistry of **1**, with the objective of performing evaluation of inhibitory activities against the production of the anti-inflammatory cytokine IL-6. IL-6 initiated signalling plays a crucial role in endothelial cell dysfunction during bacterial and viral cytokine release syndromes. IL-6 inhibitors restricting the IL-6 signalling possibly reduce inflammation and help the immune system fight the COVID-19 virus infection.<sup>7</sup> In this paper, we present the results of these studies.

## Results and discussion

Our strategy involves the synthesis of four possible candidates (**3a–d**); comparing the NMR data, optical rotation and chroma-

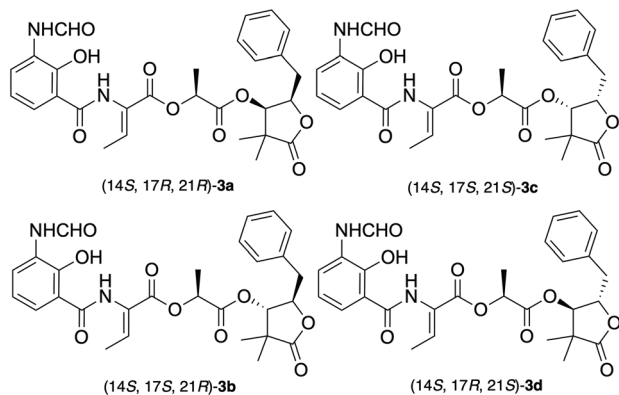


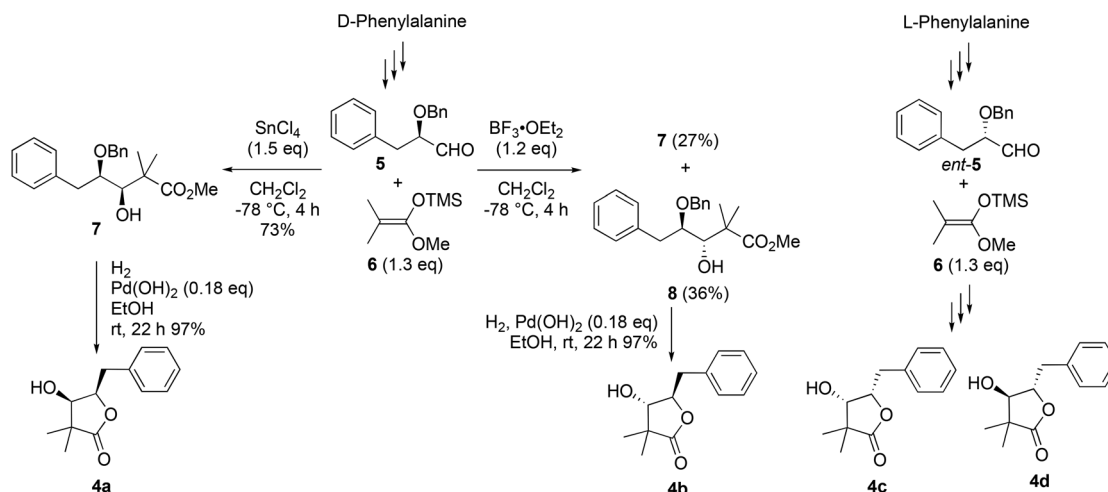
Fig. 2 Four possible candidates (**3a–d**).

tographic profiles of synthetic compounds **3a–d** to those reported for natural sample **1** would verify the absolute configuration of **1** (Fig. 2).

Previously, we have reported the preparation of (*R,R*)- $\gamma$ -butyrolactone **4a**, as shown in Scheme 1.<sup>3</sup> The use of monodentate  $\text{BF}_3 \cdot \text{Et}_2\text{O}$  instead of bidentate  $\text{SnCl}_4$  as a Lewis acid in the Mukaiyama aldol reaction of aldehyde **5**<sup>8</sup> from *D*-phenylalanine with silyl ketene acetal **6** switched *syn-anti*-selectivity;<sup>9</sup> *anti*-isomer **8** was preferentially obtained in 36% yield. The removal of the benzyl ether protecting group of **8** was achieved with a catalytic amount of  $\text{Pd}(\text{OH})_2$  in EtOH under a hydrogen atmosphere, followed by spontaneous intramolecular transesterification. (*S,R*)- $\gamma$ -Butyrolactone **4b** was thus obtained in 91% yield. The complementary enantiomers (*S,S*)-**4c** and (*R,S*)-**4d** were also prepared from *L*-phenylalanine accordingly (see details in the ESI†).

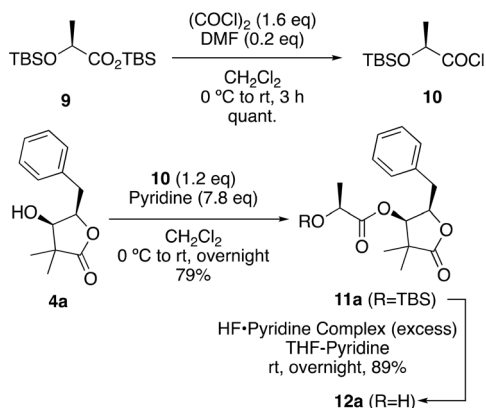
With  $\gamma$ -butyrolactones (**4a–d**) to access all possible candidates in hand, we focused on the linear assembly of each fragment. Bis-TBS protected **9**, prepared from lithium *L*-lactate,<sup>10</sup> was treated with oxalyl chloride and a catalytic amount of DMF to produce the corresponding acid chloride **10**.<sup>11</sup> The condensation of **4a** with **10** and the following deprotection of the TBS group by the HF-pyridine complex provided **12a** in good yield (Scheme 2).

The condensation of **12a** and  $\alpha$ -azido- $\alpha$ ,  $\beta$ -unsaturated acid **13**,<sup>12</sup> prepared from ethyl 2,3-dibromobutyrate, with DCC and DMAP provided the corresponding **14a** in 84% yield (Scheme 3). The preparation of **16** was achieved by the condensation of commercially available (2-hydroxyphenyl) diphenylphosphine with 3-formylaminosalicylic acid **15**<sup>13</sup> in a modest yield. Finally, we found that the traceless Staudinger ligation<sup>14</sup> of **14a** with **16** in aqueous THF successfully furnished (14*S*,17*R*,21*R*)-**3a** in 59% yield ( $[\alpha]_D^{25} +42$ ,  $c$  0.03, MeOH).<sup>15</sup> Other stereoisomers (14*S*,17*S*,21*R*)-**3b**, (14*S*,17*S*,21*S*)-**3c** and (14*S*,17*R*,21*S*)-**3d** were prepared in the same manner as shown in the ESI.†

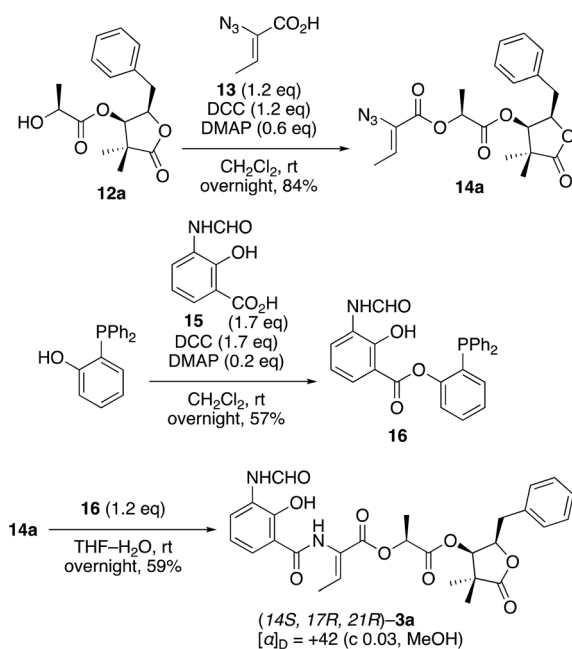


Scheme 1 Preparation of  $\gamma$ -butyrolactones **4a–d**.





Scheme 2 Synthesis of fragment 12.

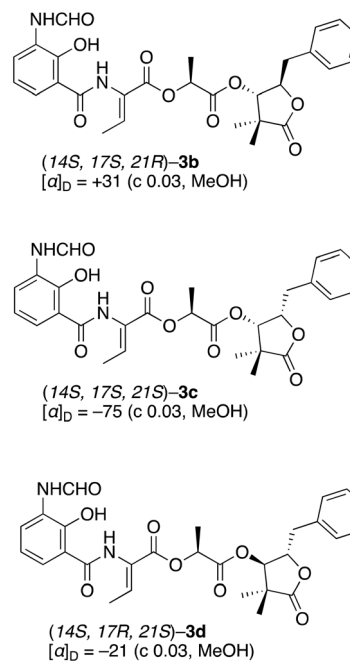


Scheme 3 Completion of the synthesis of 3a.

During the synthesis of target compounds **3a–d**, the moderate yield of the traceless Staudinger ligation would be attributed to the steric hindrance between phosphine **16** and azide **14**, which slowed the elimination of  $N_2$  from the phosphazide intermediate. This delay promoted side reactions and led to the formation of a primary amide as a byproduct.<sup>14c</sup>

The spectral data of synthetic products **3a–d** were compared with those reported for natural product **1** (Tables S1–4<sup>†</sup>); the <sup>1</sup>H NMR spectra of synthetic **3a** were almost identical to those of the natural product (Fig. S1<sup>†</sup>). The optical rotation of synthetic product **3a** ( $[\alpha]_D +42$ ,  $c$  0.03, MeOH) was in good agreement with that of the natural sample ( $[\alpha]_D +60$ ,  $c$  0.03, MeOH). Furthermore, HPLC analysis of natural product **1** and all synthetic products **3a–d** was performed. We found that the retention time ( $t_R$ ) of **3a** was identical to that of natural product **1**

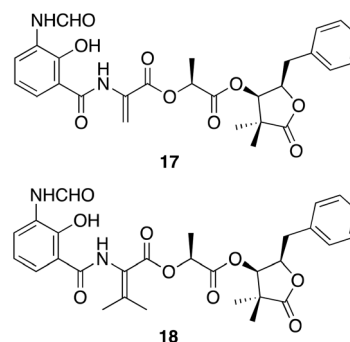
( $t_R = 6.872$  min, Fig. S3<sup>†</sup>). These data revealed that the absolute configuration of natural opantimycin A (**1**) is 14*S*,17*R*,21*R*.



With both synthetic and natural opantimycin A in hand, we evaluated their respiratory inhibitory and anti-malarial activities. Partial inhibition was observed at a concentration of 30  $\mu$ M in a Mito Stress assay using HeLa cells for both compounds **1** and **3a**. Synthetic compound **3a** exhibited similar activity to natural compound **1** against *Plasmodium falciparum* strain 3D7.

Then we focused on the evaluation of inhibitory activities against the production of the anti-inflammatory cytokine IL-6. Two analogous compounds **17** and **18** were prepared. The Dhb ((*Z*)-dehydrobutyrine) moiety was replaced by Dha (dehydroalanine) and  $\Delta$ Val moieties, respectively (Fig. 3).

The effects on the cytokine IL-6 gene suppression and RAW264 cell viability of compounds **3a–d**, **17** and **18** were evaluated. The gene expression of IL-6 was induced by lipopolysaccharide. Significant gene suppression was observed for com-

Fig. 3 Two analogous compounds (**17** and **18**).

pounds **3b** and **17** at 20  $\mu\text{M}$ , but not for the others (**3b**:  $66 \pm 2.5\%$  and **17**:  $67 \pm 2.0\%$ ; relative to the control ( $p < 0.05$ ), Fig. S4†). In contrast, the gene expression slightly increased for antimycin A (**2b**), **3a** and **3d**, supported by a previous report on antimycin A.<sup>16</sup> The typical results of cell viability tests against RAW264 cell lines were **2b**:  $69 \pm 1.9\%$ , **3b**:  $82 \pm 0.9\%$ , **3d**:  $72 \pm 2.1\%$ , and **17**:  $82 \pm 1.6\%$  at 20  $\mu\text{M}$  (Fig. S5†). These results suggest that cytotoxicity and gene suppression are not correlated.

## Conclusions

In summary, syntheses of four possible candidates **3a–d** have been achieved. A comparison of the spectroscopic data between **3a–d** and natural product **1** verified that the absolute configuration of **1** is (14*S*,17*R*,21*R*). Compounds **3b** and **17** are potential candidates for further development of anti-inflammatory agents. Further biological activity studies are ongoing, and results will be reported in due course.

## Experimental

### General information and materials

<sup>1</sup>H NMR and <sup>13</sup>C NMR spectra were recorded on a Bruker BioSpin AVANCE III HD 400 (400 MHz) or JEOL JNM-ECZ400S (400 and 100 MHz) or Bruker Avance III 600 (600 and 150 MHz) instrument. <sup>31</sup>P NMR spectra were recorded on a Bruker BioSpin AVANCE III HD 400 (121 MHz) instrument. Data are reported as follows: chemical shift, multiplicity (s = singlet, d = doublet, t = triplet, q = quartet, m = multiplet and br = broad), coupling constant in Hz, and integration. Coupling constants were determined directly from <sup>1</sup>H NMR and <sup>13</sup>C NMR spectra. The chemical shifts are reported in  $\delta$  (ppm) values relative to CHCl<sub>3</sub> ( $\delta$  7.26 ppm for <sup>1</sup>H NMR and  $\delta$  77.0 ppm for <sup>13</sup>C NMR), Me<sub>4</sub>Si ( $\delta$  0.00 ppm for <sup>1</sup>H NMR) and H<sub>3</sub>PO<sub>4</sub> ( $\delta$  0.00 ppm for <sup>31</sup>P NMR). Mass spectra were obtained on a JEOL AccuTOF LC-plus JMS-T100LP (DART, ESI) spectrometer. Infrared absorption spectra (IR) were recorded using a JASCO FT/IR-4600 Fourier transform infrared spectrometer. Optical rotations were measured on a JASCO P-2200 with a path length of 0.1 dm at ambient temperature; the concentrations are reported in g dL<sup>-1</sup>.

All air- and moisture-sensitive reactions were carried out in an argon-flushed 2-necked flask sealed with rubber septa, and dried solvents and reagents were introduced using a syringe. Tetrahydrofuran (THF) was freshly distilled under an argon atmosphere from sodium benzophenone ketyl. Flash column chromatography was carried out on a Kanto Chemical silica gel 60 N (spherical, neutral, 40–50  $\mu\text{m}$ ), and pre-coated Merck silica gel plates (Art 5715 Kieselgel 60 F<sub>254</sub>, 0.25 mm) were used for thin-layer chromatography (TLC). TLC visualization was performed using UV (254 nm) or a charring solution (ethanoic *p*-anisaldehyde and ethanoic phosphomolybdic acid).

**Methyl (4*R*,3*S*)-4-benzyloxy-3-hydroxy-2,2-dimethyl-5-phenyl-pentanoate (8).** To a solution of **5**<sup>7</sup> (180 mg, 0.749 mmol) in CH<sub>2</sub>Cl<sub>2</sub> (4 mL) was added BF<sub>3</sub>·Et<sub>2</sub>O (110  $\mu\text{L}$ , 1.05 mmol) dropwise at  $-78$  °C. After being stirred for 15 min at  $-78$  °C, commercially available dimethylketene methyl trimethylsilyl acetal **6** (180  $\mu\text{L}$ , 0.886 mmol) was added and then the mixture was stirred at  $-78$  °C for 4 h. The reaction mixture was allowed to warm up to room temperature and quenched with sat. aq. NaHCO<sub>3</sub> (6 mL). The aqueous layer was extracted with CH<sub>2</sub>Cl<sub>2</sub> (4 mL  $\times$  5). The combined organic layers were washed with brine, dried over Na<sub>2</sub>SO<sub>4</sub>, filtered and concentrated. The residue was purified by flash column chromatography (10% AcOEt in *n*-hexane) to obtain colorless oil **7**<sup>3</sup> (69.0 mg, 0.201 mmol, 27%) and **8** (80.7 mg, 0.236 mmol, 31%). Data for **8**: <sup>1</sup>H NMR (400 MHz, CDCl<sub>3</sub>)  $\delta$  7.37–7.06 (m, 10H), 4.29 (d,  $J$  = 1.7 Hz, 2H), 3.83 (t,  $J$  = 6.8 Hz, 1H), 3.66 (td,  $J$  = 6.9, 3.7 Hz, 1H), 3.40 (s, 3H), 3.11 (dd,  $J$  = 14.3, 3.7 Hz, 1H), 2.91 (dd,  $J$  = 14.3, 7.1 Hz, 1H), 2.29 (d,  $J$  = 6.8 Hz, 1H), 1.23 (s, 3H), 1.22 (s, 3H). <sup>13</sup>C NMR (150 MHz, CDCl<sub>3</sub>)  $\delta$  177.5, 139.0, 137.9, 129.8, 128.4, 128.3, 128.2, 127.6, 126.3, 81.6, 77.4, 72.3, 51.6, 45.4, 37.9, 23.8, 20.0. HRMS (DART+)  $m/z$  calcd for C<sub>21</sub>H<sub>27</sub>O<sub>4</sub> [M + H]<sup>+</sup> 343.19093, found 343.19075. IR (KBr): 3467, 2947, 1719, 1266, 1135, 1069, 748, 699 cm<sup>-1</sup>. [ $\alpha$ ]<sub>D</sub><sup>25</sup> = +20.2 (*c* 0.26 CHCl<sub>3</sub>).

**(4*S*,5*R*)-5-Benzyl-4-hydroxy-3,3-dimethylhydrofuran-2-one (4b).** To a solution of **8** (1.21 g, 3.53 mmol) in 99.5% EtOH (25 mL) was added 20% Pd(OH)<sub>2</sub> (119 mg). The inner atmosphere was purged with H<sub>2</sub>. After being stirred at room temperature for 20 h, the resulting mixture was filtered through a Celite® pad and the filtrate was concentrated. The residue was purified by flash column chromatography (30% AcOEt in *n*-hexane) to obtain white solid **4b** (729 mg, 3.31 mmol, 93%). <sup>1</sup>H NMR (400 MHz, CDCl<sub>3</sub>)  $\delta$  7.38–7.25 (m, 5H), 4.32 (ddd,  $J$  = 7.9, 6.8, 5.7 Hz, 1H), 3.87 (dd,  $J$  = 8.0, 5.3 Hz, 1H), 3.15–3.00 (m, 2H), 1.63 (d,  $J$  = 5.3 Hz, 1H), 1.23 (s, 3H), 1.16 (s, 3H). <sup>13</sup>C NMR (100 MHz, CDCl<sub>3</sub>)  $\delta$  179.5, 136.1, 129.5, 129.0, 127.3, 81.8, 79.6, 43.8, 39.1, 22.9, 17.9. HRMS (ESI+)  $m/z$  calcd for C<sub>13</sub>H<sub>16</sub>NaO<sub>3</sub> [M + Na]<sup>+</sup> 243.09971, found 243.10111. IR (KBr): 3404, 3026, 2980, 2915, 1735, 1112, 997, 757, 698 cm<sup>-1</sup>. [ $\alpha$ ]<sub>D</sub><sup>26</sup> = +74.3 (*c* 0.38 CH<sub>2</sub>Cl<sub>2</sub>).

**(*S*)-2-(*tert*-Butyldimethylsilyloxy) propanoic acid [(4*R*,5*R*)-5-benzyl-3,3-dimethylhydrofuran-2-one-4-yl] ester (11a).** To a solution of lithium L-lactate (602 mg, 6.27 mmol) in DMF (6 mL) were added TBSCl (1.95 g, 12.9 mmol) and imidazole (1.76 g, 25.9 mmol). After being stirred at room temperature for 17 h, the resulting mixture was diluted with sat. aq. NaHCO<sub>3</sub> (25 mL) and extracted with *n*-hexane (15 mL  $\times$  3). The combined organic layers were washed with brine, dried over Na<sub>2</sub>SO<sub>4</sub>, filtered and concentrated to obtain colorless oil **9** (1.66 g, 5.21 mmol, 83%). This was used for the next reaction without further purification. <sup>1</sup>H NMR (400 MHz, CDCl<sub>3</sub>)  $\delta$  4.26 (q,  $J$  = 6.8 Hz, 1H), 1.39 (d,  $J$  = 6.8 Hz, 3H), 0.94 (s, 9H), 0.90 (s, 9H), 0.27 (s, 6H), 0.10 (s, 3H), 0.07 (s, 3H). HRMS (ESI+)  $m/z$  calcd for C<sub>15</sub>H<sub>34</sub>NaO<sub>3</sub>Si<sub>2</sub> [M + H]<sup>+</sup> 341.19442, found 341.19446. To a solution of **9** (867 mg, 2.72 mmol) in CH<sub>2</sub>Cl<sub>2</sub> (3.2 mL) were added oxalyl chloride (300  $\mu\text{L}$ , 3.82 mmol) and DMF (36  $\mu\text{L}$ , 0.46 mmol). The solution was stirred for 1 h at 0 °C



and then stirred at room temperature for 3 h. The resulting mixture was concentrated to obtain the corresponding acid chloride **10** quantitatively. To the acid chloride above prepared were added a solution of **4a** (299 mg, 1.36 mmol) in CH<sub>2</sub>Cl<sub>2</sub> (3.2 mL) and pyridine (1.15 mL) at 0 °C. After being stirred at room temperature for 13 h, the reaction mixture was quenched with sat. aq. NaHCO<sub>3</sub> (10 mL) and extracted with AcOEt (17 mL × 5). The combined organic layers were washed with sat. aq. NH<sub>4</sub>Cl and brine, dried over Na<sub>2</sub>SO<sub>4</sub>, filtered and concentrated. The residue was purified by flash column chromatography (30% AcOEt in *n*-hexane) to obtain colorless oil **11a** (448 mg, 1.10 mmol, 81%). <sup>1</sup>H NMR (400 MHz, CDCl<sub>3</sub>) δ 7.36–7.20 (m, 5H), 5.28 (d, *J* = 3.7 Hz, 1H), 4.79 (ddd, *J* = 8.6, 5.2, 3.7 Hz, 1H), 4.44 (q, *J* = 6.7 Hz, 1H), 3.09 (dd, *J* = 14.3, 8.5 Hz, 1H), 2.90 (dd, *J* = 14.3, 5.2 Hz, 1H), 1.47 (d, *J* = 6.7 Hz, 3H), 1.32 (s, 3H), 1.18 (s, 3H), 0.92 (s, 9H), 0.12 (s, 3H), 0.10 (s, 3H). <sup>13</sup>C NMR (100 MHz, CDCl<sub>3</sub>) δ 179.4, 173.2, 136.3, 129.2, 128.9, 127.2, 80.1, 77.9, 68.3, 45.0, 35.2, 25.8, 22.8, 21.6, 18.4, 18.2, –4.7, –5.0. HRMS (DART+) *m/z* calcd for C<sub>22</sub>H<sub>35</sub>O<sub>5</sub>Si [M + H]<sup>+</sup> 407.22537, found 407.22540. IR (KBr) 2931, 2858, 1783, 1137, 833 cm<sup>-1</sup>. [α]<sub>D</sub><sup>25</sup> = +53.9 (*c* 0.54 CHCl<sub>3</sub>).

**(S)-2-Hydroxypropanoic acid [(4R,5R)-5-benzyl-3,3-dimethylhydrofuran-2-one-4-yl] ester (12a).** To a solution of **11a** (538 mg, 1.32 mmol) in THF (10 mL) were added pyridine (3.1 mL) and HF–pyridine (5.1 mL). After being stirred at room temperature for 15 h, the reaction mixture was quenched with sat. aq. NaHCO<sub>3</sub> (130 mL) and extracted with AcOEt (45 mL × 5). The combined organic layers were washed with brine, dried over Na<sub>2</sub>SO<sub>4</sub>, filtered and concentrated. The residue was purified by flash column chromatography (40% AcOEt in *n*-hexane) to obtain white solid **12a** (307 mg, 1.05 mmol, 80%). <sup>1</sup>H NMR (400 MHz, CDCl<sub>3</sub>) δ 7.50–7.07 (m, 5H), 5.31 (d, *J* = 3.8 Hz, 1H), 4.83 (ddd, *J* = 8.9, 5.4, 3.8 Hz, 1H), 4.41 (p, *J* = 6.8 Hz, 1H), 3.10 (dd, *J* = 14.3, 8.4 Hz, 1H), 2.87 (dd, *J* = 14.4, 5.4 Hz, 1H), 2.65 (d, *J* = 5.6 Hz, 1H), 1.49 (d, *J* = 6.9 Hz, 3H), 1.34 (s, 3H), 1.19 (s, 3H). <sup>13</sup>C NMR (100 MHz, CDCl<sub>3</sub>) δ 179.1, 174.8, 136.0, 129.1, 128.9, 127.3, 79.8, 78.7, 66.9, 44.9, 35.2, 22.8, 20.6, 18.1. HRMS (DART+) *m/z* calcd for C<sub>16</sub>H<sub>21</sub>O<sub>5</sub> [M + H]<sup>+</sup> 293.13890, found 293.13906. IR (KBr) 2987, 2938, 1774, 1742, 1195, 1130, 1058, 722, 599 cm<sup>-1</sup>. [α]<sub>D</sub> = +80.3 (*c* 0.44 CHCl<sub>3</sub>).

**(Z)-2-Azido-2-butenic acid [(2S)-propanoic acid [(4R,5R)-5-benzyl-3,3-dimethylhydrofuran-2-one-4-yl] ester (14a).** To a solution of **13**<sup>11</sup> (15.7 mg, 0.124 mmol) and **12a** (29.5 mg, 0.100 mmol) in CH<sub>2</sub>Cl<sub>2</sub> (1.0 mL) were added DCC (25.0 mg, 0.121 mmol) and DMAP (7.7 mg, 0.063 mmol) in this order. After being stirred overnight at room temperature, the resulting mixture was filtered through a Celite® pad and the filtrate was concentrated. The residue was purified by flash column chromatography (15% AcOEt in *n*-hexane) to obtain colorless amorphous **14a** (33.7 mg, 0.0840 mmol, 84%). <sup>1</sup>H NMR (400 MHz, CDCl<sub>3</sub>) δ 7.35–7.25 (m, 5H), 6.40 (q, *J* = 9.6 Hz, 1H), 5.30 (d, *J* = 4.7 Hz, 1H), 5.29 (q, *J* = 9.7 Hz, 1H), 4.79 (ddd, *J* = 11.4, 6.6, 4.9 Hz, 1H), 3.11 (dd, *J* = 19.3, 11.3 Hz, 1H), 2.94 (dd, *J* = 19.4, 6.6 Hz, 1H), 1.84 (d, *J* = 9.6 Hz, 3H), 1.63 (d, *J* = 9.5 Hz, 3H), 1.32 (s, 3H), 1.18 (s, 3H). <sup>13</sup>C NMR (100 MHz, CDCl<sub>3</sub>) δ 178.9, 169.5, 161.8, 136.1, 129.1, 128.7, 128.4, 127.8, 127.0,

80.0, 78.7, 69.3, 44.7, 35.0, 22.6, 18.0, 17.0, 13.1. HRMS (ESI+) *m/z* calcd for C<sub>20</sub>H<sub>23</sub>N<sub>3</sub>NaO<sub>6</sub> [M + Na]<sup>+</sup> 424.14845, found 424.14479. IR (KBr): 2988, 2941, 2132, 1783, 1720, 1638, 1131, 745 cm<sup>-1</sup>. [α]<sub>D</sub> = +21.9 (*c* 0.79, CHCl<sub>3</sub>).

**3-Formylaminosalicylic acid [(2-hydroxyphenyl)diphenylphosphine] ester (16).** To a solution of 3-formylaminosalicylic acid **15**<sup>12</sup> (109.7 mg, 0.606 mmol) and commercially available (2-hydroxyphenyl)diphenylphosphine (99.6 mg, 0.358 mmol) in CH<sub>2</sub>Cl<sub>2</sub> (1.8 mL) were added DCC (125.3 mg, 0.600 mmol) and DMAP (10.0 mg, 0.082 mmol). The inner air was purged with Ar. After being stirred at room temperature overnight, the resulting mixture was filtered using a Celite® pad and the filtrate was concentrated. The residue was purified by flash column chromatography (30% AcOEt in *n*-hexane) to obtain white solid **16** (90.6 mg, 0.205 mmol, 57%). <sup>1</sup>H NMR (400 MHz, CDCl<sub>3</sub>) δ 10.75 (s, 1H), 7.85 (s, 1H), 7.33–7.29 (m, 10H), 7.25–7.20 (m, 3H), 6.91 (ddd, *J* = 7.7, 4.3, 1.6 Hz, 1H), 6.79 (t, *J* = 8.0 Hz, 1H). <sup>13</sup>C NMR (100 MHz, CDCl<sub>3</sub>) δ 168.2, 158.9, 151.7 (d, <sup>1</sup>*J*<sub>CP</sub> = 16.8 Hz), 150.5, 134.8 (d, <sup>1</sup>*J*<sub>CP</sub> = 9.6 Hz), 134.1 (d, <sup>2</sup>*J*<sub>CP</sub> = 20.7 Hz), 133.7 (d, <sup>3</sup>*J*<sub>CP</sub> = 2.3 Hz), 131.1 (d, <sup>2</sup>*J*<sub>CP</sub> = 16.0 Hz), 129.9, 129.2, 128.6 (d, <sup>3</sup>*J*<sub>CP</sub> = 7.5 Hz), 126.8, 126.3, 126.2, 124.9, 122.4, 119.2, 111.1. <sup>31</sup>P NMR (121 MHz, CDCl<sub>3</sub>) δ –15.4. HRMS (ESI+) *m/z* calcd for C<sub>26</sub>H<sub>20</sub>NNaO<sub>4</sub>P [M + Na]<sup>+</sup> 464.09421, found 464.09858. IR (KBr): 3384, 3068, 2879, 1686, 1525, 1435, 1338, 1294, 1249, 1189, 1131, 1115, 747, 697 cm<sup>-1</sup>.

**2-(3-Formylamino-2-hydroxy benzoylamino)-(Z)-2-butenic acid [(2S)-propanoic acid [(4R,5R)-5-benzyl-3,3-dimethylhydrofuran-2-one-4-yl] ester-2-yl] ester (3a).** To **14a** (33.7 mg, 0.0840 mmol) in a two-necked flask were added **16** (43.4 mg, 0.0983 mmol) in THF (3.4 mL) and water (1.2 mL). After being stirred overnight at room temperature, the resulting mixture was diluted with brine (20 mL). The aqueous layer was extracted with AcOEt (10 mL × 2). The combined organic layer was dried over Na<sub>2</sub>SO<sub>4</sub>, filtered and concentrated. The residue was purified by flash column chromatography (40% AcOEt in *n*-hexane) to obtain pale yellow amorphous **3a** (26.5 mg, 0.0493 mmol, 59%) as a 6.5 : 1 mixture of rotamers. <sup>1</sup>H NMR (600 MHz, CDCl<sub>3</sub>) major δ 12.56 (s, 1H), 8.52 (dd, *J* = 8.0, 1.3 Hz, 1H), 8.47 (d, *J* = 1.8 Hz, 1H), 7.98 (brs, 1H), 7.85 (brs, 1H), 7.32 (d, *J* = 8.4 Hz, 1H), 7.29 (t, *J* = 7.5 Hz, 1H), 7.25–7.22 (m, 2H), 7.10 (q, *J* = 7.1 Hz, 1H), 6.89 (t, *J* = 8.1 Hz, 1H), 5.30 (d, *J* = 3.0 Hz, 1H), 5.29 (q, *J* = 7.2 Hz, 1H), 4.78 (dt, *J* = 8.6, 4.2 Hz, 1H), 3.07 (dd, *J* = 14.5, 8.9 Hz, 1H), 2.89 (dd, *J* = 14.5, 4.5 Hz, 1H), 1.89 (d, *J* = 7.2 Hz, 3H), 1.61 (d, *J* = 7.1 Hz, 3H), 1.31 (s, 3H), 1.17 (s, 3H); minor (diagnostic peaks only) δ 12.42 (s, 1H), 8.76 (d, *J* = 11.5 Hz, 1H). <sup>13</sup>C NMR (150 MHz, CDCl<sub>3</sub>) δ 179.0, 169.7, 168.5, 163.4, 159.1, 150.7, 137.4, 136.2, 129.1, 128.7, 127.3, 127.0, 124.8, 124.7, 120.7, 118.9, 113.1, 80.0, 78.7, 69.3, 44.8, 35.1, 22.6, 18.0, 17.0, 14.9. HRMS (ESI+) *m/z* calcd for C<sub>28</sub>H<sub>30</sub>N<sub>2</sub>NaO<sub>9</sub> [M + Na]<sup>+</sup> 561.18490, found 561.18406. IR (KBr): 3354, 2985, 2924, 1763, 1686, 1527, 1262, 1133, 744 cm<sup>-1</sup>. [α]<sub>D</sub> = +42 (*c* 0.03, MeOH).

### Cytotoxicity assay

RAW264 cells were seeded on 96-well plates at an initial density of 5 × 10<sup>4</sup> cells per well and incubated under 5% CO<sub>2</sub>



at 37 °C for 24 h. After incubation, the cells were further incubated in Dulbecco's modified Eagle's medium containing 10% inactivated fetal bovine serum with or without each compound for 5 h. After incubation, the supernatant was removed and a Cell Counting Kit-8 (Dojindo Molecular Technologies) solution diluted with the medium was added. After a further 1 h incubation, the cell proliferation rate was estimated against the control by measuring the absorbance at 450 nm. Data represent the mean  $\pm$  SE of at least three independent experiments.

### Evaluation of IL-6 gene suppression

RAW264 cells were inoculated into a 24-well plate ( $2.5 \times 10^5$  cells per well) and cultured overnight. After cultivation, the supernatant was removed and the medium with  $100 \text{ ng mL}^{-1}$  lipopolysaccharide and test compounds was added. The cells were further incubated for 5 h. Incubation without test compounds was performed in the same manner as the control. Quercetin ( $25 \mu\text{M}$ ) was used as a positive control.<sup>17</sup> A blank was also prepared by adding only the medium. After incubation, total RNA was extracted from the cells using RNeasy (Qiagen) and cDNA was synthesized using a random primer (TaKaRa) and PrimeScript Reverse Transcriptase (TaKaRa). Using cDNA obtained as a template, Fast SYBR Green Master Mix (Applied Biosystems) and IL-6 and GAPDH specific primers (TaKaRa), real-time PCR was performed to quantify the mRNA expression levels of IL-6. The ratio of the gene expression of IL-6 to GAPDH, which was used as an internal standard, was calculated to estimate the relative expression level to the control. Data represent the mean  $\pm$  SE of at least three independent experiments.

### Statistical analysis

Statistical analysis was performed using Student's *t*-test and *p* < 0.05 was considered to represent statistical significance.

## Author contributions

Conceptualization: Yoshinosuke Usuki; data curation: Yoshinosuke Usuki; investigation: Ryota Abe and Kazuki Nishiguchi; formal analysis: Harumi Aono, Izumi Yoshida and Takashi Mishima; resource: Tetsuya Satoh; project administration: Yoshinosuke Usuki, Kazuhiro Fujita and Yushi Futamura; writing – original draft preparation: Yoshinosuke Usuki; writing – review and editing: Toshihiko Nogawa, Yushi Futamura, Hiroyuki Osada and Ken-Ichi Fujita; funding acquisition: Yoshinosuke Usuki. All authors read and approved the final manuscript.

## Data availability

The data supporting this article have been included as part of the ESI.†

## Conflicts of interest

There are no conflicts to declare.

## Acknowledgements

This work was financially supported by a Grant-in-Aid for Scientific Research (C) (No. 22K06666). We are grateful to Dr Matsumi Doe, Analytical Division, Osaka Metropolitan University, for the 2D NMR measurements.

## References

- 1 T. Nogawa, A. Okano, C. L. Lim, Y. Futamura, T. Shimizu, S. Takahashi, D. Ibrahim and H. Osada, *J. Antibiot.*, 2017, **70**, 222.
- 2 For a recent review, see: J. Liu, X. Zhu, S. J. Kim and W. Zhang, *Nat. Prod. Rep.*, 2016, **33**, 1146.
- 3 Y. Usuki, Y. Tanaka, M. Morii and T. Satoh, *Org. Biomol. Chem.*, 2023, **21**, 2398.
- 4 (a) C. J. Barrow, J. J. Oleynek, V. Marinelli, H. H. Sun, P. Kaplita, D. M. Sedlock, A. M. Gillum, C. C. Chadwick and R. Cooper, *J. Antibiot.*, 1997, **50**, 729; (b) S. P. Tzung, K. M. Kim, G. Basanez, C. D. Giedt, J. Simon, J. Zimmerberg, K. Y. Zhang and D. M. Hockenbery, *Nat. Cell Biol.*, 2001, **3**, 183; (c) L. S. Huang, D. Cobessi, E. Y. Tung and E. A. Berry, *J. Mol. Biol.*, 2005, **351**, 573; (d) X. Lin, Y. Zhou, L. Liu, H. Zhu, Y. Chen, S. Wang, F. Sun, L. Chai, B. Liu, S. Xu and H.-W. Lin, *Front. Chem.*, 2019, **7**, 481; (e) J. Seidel, Y. Miao, W. Porterfield, W. Cai, X. Zhu, S. J. Kim, F. Hu, S. Bhattarai-Kline, W. Min and W. Zhang, *Chem. Commun.*, 2019, **55**, 9379.
- 5 (a) Y. Umeda, S. Chijiwa, K. Furihata, S. Sakuda, H. Nagasawa, H. Watanabe and K. Shin-ya, *J. Antibiot.*, 2005, **58**, 206; (b) M. Izumikawa, J. Y. Ueda, S. Chijiwa, M. Takagi and K. Shin-ya, *J. Antibiot.*, 2007, **60**, 640; (c) A. A. Salim, K. J. Cho, L. Tan, M. Quezada, E. Lacey, J. F. Hancock and R. J. Capon, *Org. Lett.*, 2014, **16**, 5036.
- 6 (a) Y. Usuki, H. Ogawa, K.-I. Yoshida, T. Inaoka and H. Iio, *Asian J. Org. Chem.*, 2015, **4**, 737; (b) H. Ogawa, H. Iio and Y. Usuki, *Chem. Lett.*, 2015, **44**, 1214; (c) Y. Usuki, C. Hamada and T. Satoh, *Org. Biomol. Chem.*, 2017, **15**, 7346; (d) Y. Usuki, S. Ishii, M. Ijiri, K.-I. Yoshida, T. Satoh, S. Horigome, I. Yoshida, T. Mishima and K.-I. Fujita, *J. Nat. Prod.*, 2018, **81**, 2590; (e) C. Hamada, Y. Usuki, D. Takeuchi, H. Ogawa, R. Abe and T. Satoh, *Org. Lett.*, 2019, **21**, 965.
- 7 S. Kang, T. Tanaka, H. Inoue, C. Ono, S. Hashimoto, Y. Kioi, H. Matsumoto, H. Matsuura, T. Matsubara, K. Shimizu, H. Ogura, Y. Matsuura and T. Kishimoto, *Proc. Natl. Acad. Sci. U. S. A.*, 2020, **117**, 22351.
- 8 (a) H. W. Yang and D. Romo, *J. Org. Chem.*, 1998, **63**, 1344; (b) H. Lubin, A. Tessier, G. Chaume, J. Pytkowicz and T. Brigaud, *Org. Lett.*, 2010, **12**, 1496.



- 9 For a review on the Mukaiyama aldol reaction, see: J.-I. Matsuo and M. Murakami, *Angew. Chem., Int. Ed.*, 2013, **52**, 9109.
- 10 S. L. Less, S. Handa, K. Millburn, P. F. Leadlay, C. J. Dutton and J. Staunton, *Tetrahedron Lett.*, 1996, **37**, 3515.
- 11 A. Wissner and C. V. Grudzinskas, *J. Org. Chem.*, 1978, **43**, 3972.
- 12 (a) M. Kakimoto, K. Mariko and K. Kondo, *Chem. Lett.*, 1982, **11**, 525; (b) T. Yamashita, H. Matoba, T. Kuranaga and M. Inoue, *Tetrahedron*, 2014, **70**, 7746.
- 13 G. R. Pettit, T. H. Smith, S. Feng, J. C. Knight, R. Tan, R. K. Pettit and P. A. Hinrichs, *J. Nat. Prod.*, 2007, **70**, 1073.
- 14 (a) E. Saxon, J. I. Armstrong and C. R. Bertozzi, *Org. Lett.*, 2000, **2**, 2141; (b) B. L. Nilsson, L. L. Kiessling and R. T. Raines, *Org. Lett.*, 2000, **2**, 1939; (c) For a recent example of traceless Staudinger ligation in a total synthesis, see: H. Itoh, K. Miura, K. Kamiya, T. Yamashita and M. Inoue, *Angew. Chem., Int. Ed.*, 2020, **59**, 4564.
- 15 The  $^1\text{H}$  and  $^{13}\text{C}$  NMR spectra indicated that synthetic compound **3** existed as a *ca.* 6 : 1 mixture of two rotamers. This phenomenon was also observed in the total synthesis of isoneoantimycin.<sup>3</sup>
- 16 K. Sasaki, K. Gotoh, S. Miake, D. Setoyama, M. Yagi, K. Igami, T. Uchiumi and D. Kang, *EBioMedicine*, 2017, **20**, 161.
- 17 J. Michaud-Levesque, N. Bousquet-Gagnon and R. Béliveau, *Exp. Cell Res.*, 2012, **318**, 925.

